Design and Development of Low Cost Variable Buoyancy System for the Soft Grounding of Autonomous Underwater Vehicles

Jeffery S. Riedel, Anthony J. Healey, David B. Marco and Bahadir Beyazay
Naval Postgraduate School
Center for AUV Research
Monterey, CA 93943-5000
408.656.1146 voice, 408.656.2238 fax
{jsriedel, healey, marco, bbeyazay}@me.nps.navy.mil

ABSTRACT

To provide a vehicle with the ability to hold position in a coastal environment requires a significant amount of onboard power. This power requirement either forces the vehicle size to increase to allow for suitable mission duration or reduces the amount of time the vehicle has to conduct its mission. To relax the power requirement, we propose to develop vehicles that can employ a bottom-sitting or soft grounding behavior. To obtain this behavior requires vehicles that have the capability to self-ballast. By optimally positioning itself and sitting on the bottom, the AUV can be placed in a sleep mode, with only monitoring sensors awake, thereby conserving power.

In this paper we present the preliminary work conducted in the areas of simulation, design and testing of a Variable Buoyancy System (VBS) for an Autonomous Underwater Vehicle (AUV). This buoyancy system will be integrated into the new NPS AUV which is currently under construction, to support the upcoming joint operations with the University of Lisbon's MARIUS vehicle. We will discuss the tradeoffs and analysis that went into the design of the system, as well as the challenges associated with the integration of such a behavior and system into the vehicle.

INTRODUCTION

Energy storage is limited in AUV's. To assist with energy management, data gathering missions have been proposed where the vehicle should sit on the bottom and gather acoustic/video/chemical data over extended periods of time. In this grounding scenario, thrusters may be used. However, there are two disadvantages for this method: high energy consumption and restricted use close to the ocean bottom. The motivation for this paper is to study a low cost, simple soft grounding capability for a submersible vehicle using controllable ballast. For simplicity, water ballast is considered. The design of the control system is based on the NPS Phoenix AUV. The ballast system is designed to control the weight addition into or out of the two ballast tanks.

Ballast control of vehicles is not a new subject and we can find many examples beginning in the 1900's, the non-rigid airships are very good examples of ballast control. One of the most important elements of a non-rigid airship is the ballonet-system. A ballonet as seen in Figure 1 is an airbag (one or two of them) inside the envelope, which is provided with air from a blower or directly from the engine unit. The air could be removed from the ballonet through the valves. If the airship has a front and aft ballonet then the height and pitch of the airship can be steered. For example, if the aft bag is filled with more air, then the airship will become heavier in the rear part of the envelope and the ship will incline increasing the altitude of the ship by using the engines. As Figure 1 depicted, the airship can also be statically trimmed [1]. Control was manual.

For most underwater vehicles, the depth / pitch control is normally provided by hydroplanes. As an example, consider the NPS Phoenix AUV, the MIT Odyssey and the WHOI Remus. At low speed however, the control surfaces provide reduced control authority and the ballast control problem is very complex due to nonlinear, time-varying, uncertain hydrodynamics. Inherent lags arising from the integration of ballast water flow rate commands into weight change makes the control difficult to stabilize. There are some designs that used a bang-bang control system [2]. The ARPA's Unmanned Undersea Vehicle (UUV) employed a fuzzy logic ballast controller which was claimed to be comparable with the performance that can be obtained from standard control techniques, but does not require traditional linear or nonlinear design methods.

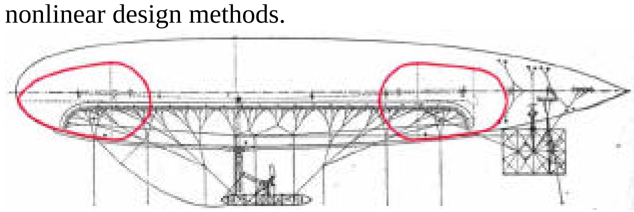

Figure 1. Sectional elevation of the Parseval-Airship "PL VI", 1910.

Report Documentation Page

Form Approved
OMB No. 0704-0188

1. REPORT DATE **2005**	2. REPORT TYPE	3. DATES COVERED **-**
4. TITLE AND SUBTITLE **Design and Development of Low Cost Variable Buoyancy System for the Soft Grounding of Autonomous Underwater Vehicles**		5a. CONTRACT NUMBER 5b. GRANT NUMBER 5c. PROGRAM ELEMENT NUMBER
6. AUTHOR(S)		5d. PROJECT NUMBER 5e. TASK NUMBER 5f. WORK UNIT NUMBER
7. PERFORMING ORGANIZATION NAME(S) AND ADDRESS(ES) **Naval Postgraduate School,Center for AUV Research,Monterey,CA,93943-5000**		8. PERFORMING ORGANIZATION REPORT NUMBER
9. SPONSORING/MONITORING AGENCY NAME(S) AND ADDRESS(ES)		10. SPONSOR/MONITOR'S ACRONYM(S) 11. SPONSOR/MONITOR'S REPORT NUMBER(S)

12. DISTRIBUTION/AVAILABILITY STATEMENT
Approved for public release; distribution unlimited

13. SUPPLEMENTARY NOTES
The original document contains color images.

14. ABSTRACT
To provide a vehicle with the ability to hold position in a coastal environment requires a significant amount of onboard power. This power requirement either forces the vehicle size to increase to allow for suitable mission duration or reduces the amount of time the vehicle has to conduct its mission. To relax the power requirement, we propose to develop vehicles that can employ a bottom-sitting or soft grounding behavior. To obtain this behavior requires vehicles that have the capability to selfballast. By optimally positioning itself and sitting on the bottom, the AUV can be placed in a sleep mode, with only monitoring sensors awake, thereby conserving power. In this paper we present the preliminary work conducted in the areas of simulation, design and testing of a Variable Buoyancy System (VBS) for an Autonomous Underwater Vehicle (AUV). This buoyancy system will be integrated into the new NPS AUV which is currently under construction, to support the upcoming joint operations with the University of Lisbon's MARIUS vehicle. We will discuss the tradeoffs and analysis that went into the design of the system, as well as the challenges associated with the integration of such a behavior and system into the vehicle.

15. SUBJECT TERMS

16. SECURITY CLASSIFICATION OF:			17. LIMITATION OF ABSTRACT	18. NUMBER OF PAGES	19a. NAME OF RESPONSIBLE PERSON
a. REPORT **unclassified**	b. ABSTRACT **unclassified**	c. THIS PAGE **unclassified**		**12**	

In another fuzzy logic control model, a 15 state Kalman filter was developed to provide estimates of the motion variables and the applied lift and torque acting on the UUV. The control law decided between three possible control actions; pump water in both tanks, pump water out of both tanks and turn both pumps off. The fuzzy input state space was composed of depth error and depth rate, and each is divided into partitions. The fuzzy controller interpolated between the partitions allowing the control to vary smoothly as the states move from one partition to another. These movements of states were provided by on and off of ballast pumps [3].

In this paper we outline the development of a depth controller using sliding mode control techniques for a neutrally buoyant vehicle. The sliding mode controller is designed on the basis of the simplified four degrees of freedom vertical plane equations of motion. A linear quadratic regulator (LQR) proportional approach is then utilized for the design of the ballast controller, which produces flow rate commands, allowing the vehicle to have a soft grounding behavior. These two controllers use a logic based depth regulator to provide realistic simulation of the vehicle's flight and grounding operations in a single mission.

VEHICLE MODELING AND EQUATIONS OF MOTION

We will deal with only vertical plane variables; i.e., heave, pitch, and surge. The vertical plane stability analysis involves heave and pitch motions. However, the surge equation couples into pitch and heave through the offset, z_G. This is a dynamic coupling, and could be eliminated by redefining hydrodynamic coefficients with respect to the ship's center of gravity instead of its geometric center.

Restricting the motions of the vehicle to the vertical (dive) plane, the only significant motions that must be incorporated to model the vehicle in the dive plane are, the surge velocity (u), the heave velocity (w), the pitch velocity (q), the pitch angle (θ) and the global depth position (*Z*).

$$\dot{\theta} = q$$

$$(-mx_G - M_{\dot{w}})\dot{w} + (I_y - M_{\dot{q}})\dot{q} = (M_q - mx_G)Uq - mz_G wq$$

$$+ M_w Uw + U^2(M_{\delta_s} + \alpha M_{\delta_b})\delta_s - \frac{1}{2}\rho\int_{tail}^{nose} C_D b(x)\frac{(w-xq)^3}{|w-xq|}x\,dx -$$

$$(x_G W - x_B B)\cos\theta - (z_G W - z_B B)\sin\theta$$

$$\dot{Z} = -U\sin\theta + w\cos\theta \qquad (1)$$

These equations can be linearized for a level flight path when the following are obtained :

$$\begin{bmatrix} 1 & 0 & 0 & 0 \\ 0 & (m - Z_{\dot{w}}) & -(mx_G + Z_{\dot{q}}) & 0 \\ 0 & -(mx_G + M_{\dot{w}}) & (I_y - M_{\dot{q}}) & 0 \\ 0 & 0 & 0 & 1 \end{bmatrix} \begin{bmatrix} \dot{\theta} \\ \dot{w} \\ \dot{q} \\ \dot{Z} \end{bmatrix} =$$

$$\begin{bmatrix} 0 & 0 & 1 & 0 \\ 0 & Z_w U & (Z_q + m)U & 0 \\ -(z_G - z_B)W & M_w U & (M_q - mx_G)U & 0 \\ -U & 1 & 0 & 0 \end{bmatrix} \begin{bmatrix} \theta \\ w \\ q \\ Z \end{bmatrix} + \begin{bmatrix} 0 \\ U^2 Z_\delta \\ U^2 M_\delta \\ 0 \end{bmatrix}\delta$$

(2)

For the cases considered during this work, the vehicle has also two ballast tanks which were designed to be used during the grounding. These ballast tanks can be seen in Figure 2.

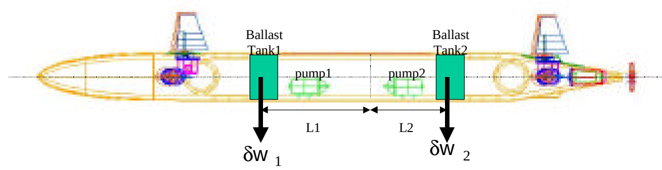

Figure 2. The Location of Ballast Tanks in the AUV

The new forces are δw_1 and δw_2 and since the ballast tanks are not located in the same distance from the center of gravity of the vehicle there will be also two moments, $L_1\delta w_1$ and $L_2\delta w_2$. There will be also small change in moment of inertia. So all these changes can be listed as;

$$W = W_o + \delta w_1 + \delta w_2$$

$$m = \frac{(W_o + \delta w_1 + \delta w_2)}{g},$$

and the new equations of motion become,

$$\boldsymbol{M} = \begin{bmatrix} 1 & 0 & 0 & 0 \\ 0 & (m - Z_{\dot{w}}) & -(mx_G + Z_{\dot{q}}) & 0 \\ 0 & (-mx_G - M_{\dot{w}}) & (I_y - M_{\dot{q}}) & 0 \\ 0 & 0 & 0 & 1 \end{bmatrix}$$

$$
\boldsymbol{A}_o = \begin{bmatrix} 0 & 0 & 1 & 0 \\ 0 & Z_w u & (m + Z_q)U & 0 \\ -(z_G W - z_B B) & M_w u & (M_q - m x_G)U & 0 \\ -u & 1 & 0 & 0 \end{bmatrix}
$$

$$
\boldsymbol{B}_o = \begin{bmatrix} 0 & 0 & 0 \\ 1 & 1 & Z_d U^2 \\ -L_1 & L_2 & M_d U^2 \\ 0 & 0 & 0 \end{bmatrix}
$$

$$
\boldsymbol{U} = \begin{bmatrix} \mathrm{d}w_1 \\ \mathrm{d}w_2 \\ \mathrm{d}_s \end{bmatrix} \quad state\_\mathrm{var}\,iables = \begin{bmatrix} \mathrm{q} \\ w \\ q \\ Z \end{bmatrix}
$$

where

$$
\dot{\boldsymbol{x}} = \boldsymbol{M^{-1}A_o x} + \boldsymbol{M^{-1}B_o u}
$$

CONTROL SYSTEM DESIGN

Flight Control

Flight control and weight control compose two main subsystem of a soft grounding system. In flight control the vehicle is kept neutrally buoyant and the plane angles are the control inputs. However in weight control, the flow rates for both ballast tanks are controlled with zero forward velocity and plane angle. These two components of the designed control system were explained in following sections.

The dynamics of underwater vehicles are described by highly nonlinear systems of equations with uncertain coefficients and disturbances that are difficult to measure. An automatic controller for this kind of vehicle must satisfy two conflicting requirements: First, it must be sophisticated enough to perform its mission in an open ocean environment with ever-changing vehicle /environment interactions. Second, it must be simple enough to achieve real-time control without nonessential computational delays. Sliding mode control theory yields a design that fulfills the above requirements. It provides accurate control of nonlinear systems despite un-modeled system dynamics and disturbances. Furthermore, a sliding mode controller is easy to design and implement. A very effective sliding mode controller can be developed from the linearized equations of motion for an underwater vehicle [7], where the control law becomes [7],

$$
\boldsymbol{u} = -\boldsymbol{kx} - (\boldsymbol{s}^T \boldsymbol{B})^{-1} \mathrm{h}\, sat\, \mathrm{sgn}(\boldsymbol{s}^T \boldsymbol{x} / \mathrm{f}\,) \tag{3}
$$

The gain vector **k** can be found easily by using Matlab. The Matlab command **place** accepts as inputs the ***A*** and ***B*** matrices along with a vector of the desired closed loop poles and returns the vector ***k***.

Weight Control

The vehicle's grounding behavior can be simulated by adding weight proportionally to both tanks at constant flow rate and by using zero plane angle. It is needed to add weight proportionally to eliminate the moment effect since these ballast tanks are not located in the same distance from the center of gravity. As it can be seen from the Figure 2, $L_1 > L_2$.

To get zero moment,

$$
\mathrm{d}w_2 = \frac{L_1}{L_2}\mathrm{d}w_1
$$

Since ballast control is achieved through commanded pump flow rate, two more state equations are added to those existing four states,

$$
\mathrm{d}\dot{w}_1 = f_1
$$

$$
\mathrm{d}\dot{w}_2 = f_2
$$

where $\mathrm{d}\dot{w}_i$ represents change of weight in tank *i* and f_i represents flow rate of pump *i*. So the ballast control equations of motion become :

$$
\begin{bmatrix} 1 & 0 & 0 & 0 & 0 & 0 \\ 0 & (m - Z_{\dot{w}}) & (-m x_G - Z_{\dot{q}}) & 0 & 0 & 0 \\ 0 & (-m x_G - M_{\dot{w}}) & (I_y - M_{\dot{q}}) & 0 & 0 & 0 \\ 0 & 0 & 0 & 1 & 0 & 0 \\ 0 & 0 & 0 & 0 & 1 & 0 \\ 0 & 0 & 0 & 0 & 0 & 1 \end{bmatrix} \begin{bmatrix} \dot{\mathrm{q}} \\ \dot{\mathrm{w}} \\ \dot{q} \\ \dot{z} \\ \mathrm{d}\dot{w}_1 \\ \mathrm{d}\dot{w}_2 \end{bmatrix}
$$

$$
= \begin{bmatrix} 0 & 0 & 1 & 0 & 0 & 0 \\ 0 & Z_w u & (m + Z_q)U & 0 & 1 & 1 \\ -(z_G W_o - z_B B) & M_w u & (M_q - m x_G)U & 0 & -L_1 & L_2 \\ -u & 1 & 0 & 0 & 0 & 0 \\ 0 & 0 & 0 & 0 & 0 & 0 \\ 0 & 0 & 0 & 0 & 0 & 0 \end{bmatrix} \begin{bmatrix} \mathrm{q} \\ \mathrm{w} \\ q \\ z \\ \mathrm{d}w_1 \\ \mathrm{d}w_2 \end{bmatrix} + \begin{bmatrix} 0 & 0 \\ 0 & 0 \\ 0 & 0 \\ 0 & 0 \\ 1 & 0 \\ 0 & 1 \end{bmatrix} \begin{bmatrix} f_1 \\ f_2 \end{bmatrix}
$$

Flow rates for ballast tanks are control inputs.

Weight Control With Linear Quadratic Regulator

The system above is given as,

$$
\dot{\boldsymbol{x}} = \boldsymbol{Ax} + \boldsymbol{Bu}
$$

and the closed loop optimal control law can be found by

$$
\boldsymbol{u} = \boldsymbol{R^{-1} B^T S x}
$$

where ***S*** can be found by solving the algebraic Riccati equation for the positive-definite S ,

$$
\boldsymbol{A^T S} + \boldsymbol{SA} - \boldsymbol{SBR^{-1} B^T S} + \boldsymbol{Q} = \boldsymbol{0}
$$

In Matlab, the command

lqr(***A***,***B***,***Q***,***R***)

gives the continuous-time, linear, quadratic regulator problem and the associated Riccati equation. This command calculates the optimal feedback gain matrix ***K*** for control law which minimizes the well known performance index.

GROUNDING WITH VERTICAL THRUSTERS

The bladed thrusters are the essential elements of improved vehicle positioning systems. With automatic position control, the thrusters enable important scientific and industrial tasks such as automatic docking, station keeping, precise surveying, inspection, sample gathering and manipulation. Incorporating precise models of thruster dynamics into the feedback control systems of marine vehicles promises improved vehicle positioning [9].

Most small-to-medium sized underwater vehicles are powered by electric motors driving propellers mounted in ducts. The propeller is mounted in a duct or shroud in order to increase the static and dynamic efficiency of the thruster. Thrusters are subject to serious degradation due to axial and cross flow effects. Axial flow effects can be reasonably approximated by the modeling of the thruster unit alone, the velocity of the fluid entering the thruster shroud effectively changes the angle of attack of the propeller , thus altering the force produced. Cross flow effects are much more difficult to model and are highly dependent on the position of the thruster on the vehicle. The amount of force produced by the thruster will reduce the overall gain of a control system unless these effects are specifically in the controller design [10].

For this work, NPS Phoenix vehicle is taken as an example. Figure 3 shows the locations of vertical and horizontal thrusters on the vehicle. Those four tubes represent the thruster shrouds. In Figure 3, the vertical thruster tubes can be seen throughout the vehicle. Thruster blades are located close to the bottom of those tubes.

Thruster moment and force equations were developed by Whitcomb and Yoerger [9], amongst others. In that paper, the control system for these thrusters was also discussed. But in this study, these thruster force and moments were assumed as some constant parameters and also no control law was developed to control them. Since the main element for grounding is the weight control, the thrusters were just used as auxiliary elements of this procedure in order to increase depth rate. By using thrusters in addition to the weight control, following changes should be made to heave and pitch rate equations,

$$(m - Z_{\dot w})\dot w + (-m x_G - Z_{\dot q})\dot q = (m + Z_q)Uq + m z_G q^2 + Z_w U w + (\delta w_1 + \delta w_2)\cos\theta$$

$$-\frac{1}{2}\rho \int_{tail}^{nose} C_D b(x)\frac{(w - xq)^3}{|w - xq|}dx + Z_{thruster}$$

$$(-m x_G - M_{\dot w})\dot w + (I_y - M_{\dot q})\dot q = (M_q - m x_G)Uq - m z_G w q + M_w U w$$

$$-\frac{1}{2}\rho \int_{tail}^{nose} C_D b(x)\frac{(w - xq)^3}{|w - xq|}x\,dx$$

$$-(x_G W_o - x_B B)\cos\theta - (z_G W - z_B B)\sin\theta + (-L_1\delta w_1 + L_2\delta w_2)\cos\theta - M_{thruster} q \quad (4)$$

where $Z_{thruster}$ and $M_{thruster}$ are thruster force and thruster moment respectively.

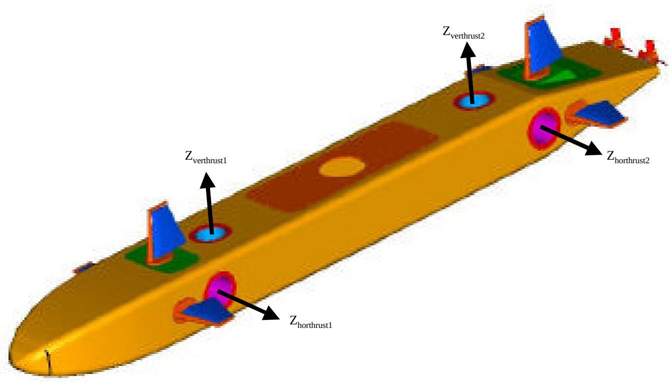

Figure 3 Horizontal and Vertical Thrusters of NPS Phoenix AUV

RESULTS AND DISCUSSION

In previous chapters, the mathematical models of the control system were developed. To prove the validity of the flight and weight controllers, the system was simulated by using the parameters of NPS Phoenix AUV. First the AUV was controlled by a flight controller (sliding mode control) during its diving from surface to a commanded flight depth. Second, the flight controller and the different cases of weight controller were simulated on the vehicle.

<u>Flight Control</u>

In the NPS Phoenix vehicle, there are four vertical control planes powered by servo motors. Using the parameters of NPS Phoenix AUV and a nominal speed of 4 ft/sec, ***A*** and ***B*** matrices become

$$\boldsymbol{A} = \begin{bmatrix} 0 & 0 & 1 & 0 \\ 0.0155 & -3.4119 & -0.9247 & 0 \\ -0.1086 & 0.6027 & -0.9667 & 0 \\ -4 & 1 & 0 & 0 \end{bmatrix} \quad \boldsymbol{B} = \begin{bmatrix} 0 \\ -0.7139 \\ -0.0123 \\ 0 \end{bmatrix}$$

By choosing the poles as p = [-2, -2.1, -2.2, 0], the vector ***k*** was calculated,

$$\boldsymbol{k} = [-18.3998 , -2.4217 , -15.6369 , 0] \quad (5.3)$$

$\boldsymbol{A}_C$ is calculated from $\boldsymbol{A}_C = \boldsymbol{A} - \boldsymbol{Bk}$

$$\boldsymbol{A}_C = \begin{bmatrix} 0 & 0 & 1 & 0 \\ -13.1205 & -5.1408 & -12.0882 & 0 \\ -0.3352 & 0.5729 & -1.1592 & 0 \\ -4.0 & 1 & 0 & 0 \end{bmatrix}$$

The eigenvector of $\boldsymbol{A}^T_C$ for the pole at the origin is the sliding surface

s = [-0.8733 ; -0.0272 ; -0.4692 ; 0.1287]

as a result with $\phi = 0.1$, the control law becomes

$$\delta = -18.3998\theta - 2.4217w - 15.6319q$$
$$-(0.4) sat\,\mathrm{sgn}\left\{\begin{bmatrix} -0.8733\theta - 0.0272w - 0.4692q + \\ 0.1287(z - z_{com}) \end{bmatrix} / 0.1\right\}. \quad (5)$$

The motion of the vehicle is restricted to the vertical plane. The motion profiles for depth and pitch have been specified using sliding mode control. For the maneuver, the commanded depth was 4 ft and the vehicle was originally at the surface. As can be seen from the Figure 4, during the flight, maximum pitch angle becomes 0.042 rad (~ 2.5 degrees). When the vehicle reaches the commanded depth as seen in Figure 5, the pitch angle becomes zero as expected . The controller produces the dive plane angle command according to the depth error. In the beginning the depth error is large, so the system produces higher values of plane angle command in order to eliminate this error. With the full state feedback, the vehicle responded very well to these commands.

<u>Adding Weight To Both Tanks Without Control</u>

After completion of the flight to the commanded depth, the vehicle gets water to both tanks in order to become heavy. Figure 6 shows the weight increase in the tanks. During grounding, the planes kept at zero degrees as depicted in Figure 7. To keep depth rate within limits, the maximum weight pumped in was limited at 5 lb. for each tank. With this additional weight, the vehicle sat on the ground (10 ft.) with 0.6 ft/sec depth rate. Even though the weight was added proportionally ($\delta w_2 = (L_1 / L_2)\delta w_1$) to get zero moment effect, there is still some moment because of the vehicle motion. As a result, the pitch angle increases since there is no control on either depth rate or pitch angle. As seen on Figure 8 and Figure 5-6, at the end of a 6 ft. drop, the pitch angle becomes 0.6 rad. (35 degrees). This method can be used for very short grounding depths (2-3 ft), but for other cases, it is not recommended since the system is completely unstable.

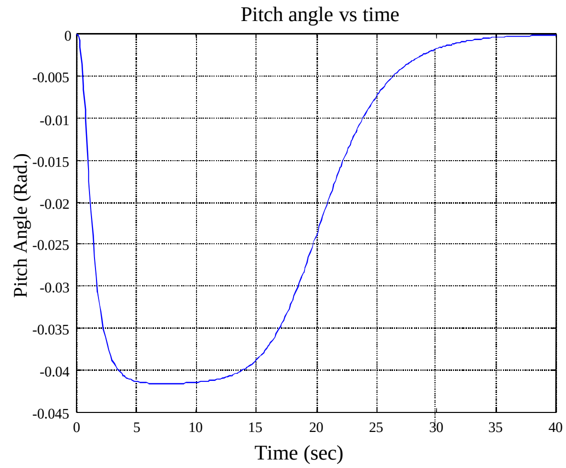

Figure 4. Pitch Angle Plot During The Flight

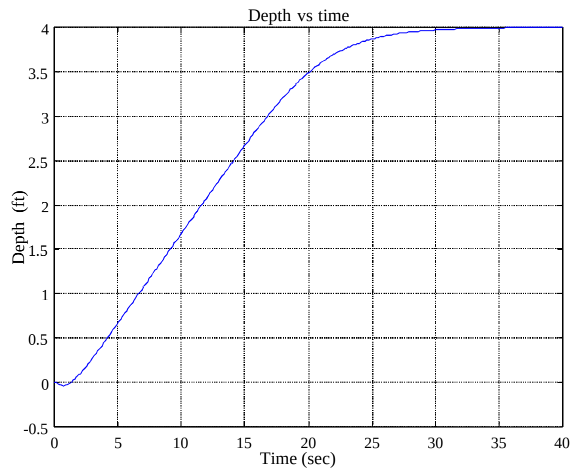

Figure 5. Depth Change As A Function Of Time During The Flight.

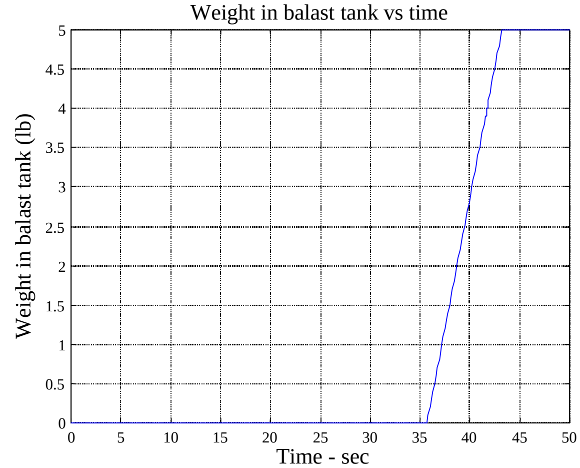

Figure 6. Weight Addition During Grounding With No Control On Flow Rates

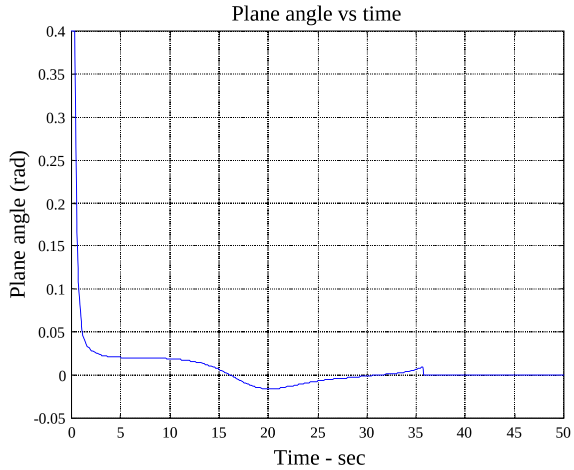

Figure 7. Plane Angle During Flight And Grounding

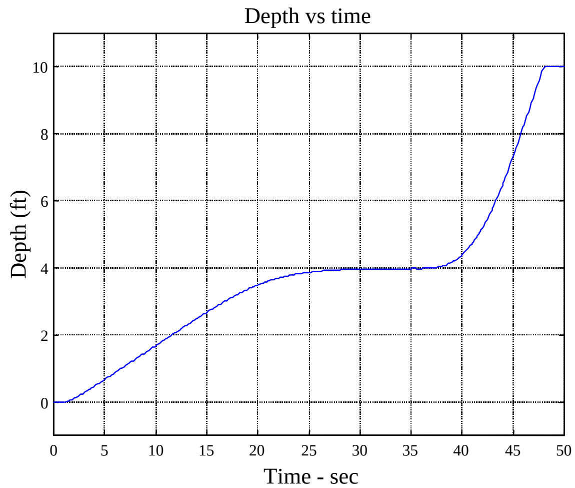

Figure 8. Depth Change During The Flight And Grounding

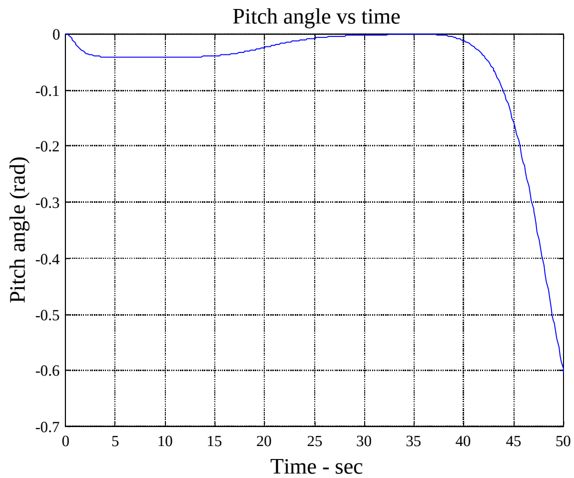

Figure 9. Pitch Angle Change For Flight And Grounding

<u>Weight Control With Linear Quadratic Regulator</u>

In order to keep the depth rate and pitch angle within limits, the linear quadratic regulator technique was used in designing a weight control. The parameters of NPS Phoenix vehicle were used for simulation. With these known parameters and 0.1 ft/sec forward velocity, ***A*** and ***B*** matrices become,

$$\boldsymbol{A} = \begin{bmatrix} 0 & 0 & 1 & 0 & 0 & 0 \\ 0.0155 & -0.0853 & -0.0231 & 0 & 0.0223 & 0.0196 \\ -0.1086 & 0.0151 & -0.0242 & 0 & -0.0130 & 0.0065 \\ -0.1 & 1 & 0 & 0 & 0 & 0 \\ 0 & 0 & 0 & 0 & 0 & 0 \\ 0 & 0 & 0 & 0 & 0 & 0 \end{bmatrix} \quad \boldsymbol{B} = \begin{bmatrix} 0 & 0 \\ 0 & 0 \\ 0 & 0 \\ 0 & 0 \\ 1 & 0 \\ 0 & 1 \end{bmatrix}$$

In practice, high values of pitch angle (> 15 degrees) are not desired for a safe and stable grounding of the vehicle. So the designed control law should not tolerate large pitch angles. Choosing larger elements of Q for the pitch angle compared with the others can provide improved control. So, the ***Q*** and ***R*** matrices were chosen as follows:

$$\boldsymbol{Q} = \begin{bmatrix} 10^4 & 0 & 0 & 0 & 0 & 0 \\ 0 & 1 & 0 & 0 & 0 & 0 \\ 0 & 0 & 1 & 0 & 0 & 0 \\ 0 & 0 & 0 & 10^2 & 0 & 0 \\ 0 & 0 & 0 & 0 & 1 & 0 \\ 0 & 0 & 0 & 0 & 0 & 1 \end{bmatrix} \qquad \boldsymbol{R} = \begin{bmatrix} 3\times10^5 & 0 \\ 0 & 3\times10^5 \end{bmatrix}$$

By using **lqr** command in Matlab, the control gain matrix ***K*** can be obtained, as

$$\boldsymbol{K} = \begin{bmatrix} 0.0608 & 0.1263 & -0.0526 & 0.0138 & 0.0754 & 0.0365 \\ -0.0322 & 0.1294 & 0.0021 & 0.0120 & 0.0365 & 0.0613 \end{bmatrix}$$

Since grounding to the ocean floor from a certain depth desired, the command matrix should be x_{com} = [0 0 0 z_{gr} 0 0]' where z_{gr} = (ground depth) - (the depth where grounding is started). So the control law becomes,

$$\boldsymbol{u} = -\boldsymbol{K}\boldsymbol{x}_{error}$$

where

$$\boldsymbol{x}_{error} = \boldsymbol{x} - \boldsymbol{x}_{com}$$

The simulation of the system with this control law can be seen in Figure 10 through Figure 17.

Positive flow rate represents water inlet to the ballast tanks, and negative flow represents the opposite. The pumps are not allowed to pump out when there is no water in ballast tanks. Figure 10 and Figure 11 show when the weight in a ballast tank and the pump flow rate become zero. This is provided by a simple controller which compares the weight in ballast tank (δw) and flow rate (f). If δw is equal to zero and flow rate is a negative number, than the control input (f) of that pump becomes zero.

At the commanded depth, the speed control unit slows down the vehicle to an almost zero forward velocity (U = 0.1 ft/sec). The speed controller's other duty is to control the longitudinal position. During the flight, the speed control unit compares the vehicle's location (X) with commanded location (X_{com}) which is a longitudinal distance from the original position. When the vehicle is at the commanded depth of flight, a deceleration procedure starts. A simple algorithm was used to calculate the minimum distance needed for deceleration to reach the commanded location at the end of the grounding. The change of forward velocity due to the depth change can be seen in the Figure 16.

The depth rate as seen in Figure 14 is very low in this method because of the command given to the weight control. The weight control produces its control values due to the errors that are the differences between the commanded and the actual states. In the above case, only the depth (Z) command has a value, the commands for other states are zero. At the end of the simulation, the pitch angle becomes almost zero as seen in Figure 15. In the first half of the grounding, Figure 12 and Figure 13 show an increase in weight for both tanks, but in the second half, the system tries to make the vehicle neutrally buoyant as expected.

LQR With Positive Weight Command

So when the vehicle reaches the ground, there will be almost no water in ballast tanks. But for the stability of the grounding, the vehicle should be heavier. For this reason, in addition to the depth command, the weight can also be commanded to increase the depth rate or the weight of the vehicle at the end of the grounding. So, the command vector, x_{com} is changed to,

$$x_{com} = [0 , 0 , 0 , z_{ground} , \delta w_{com1} , \delta w_{com2}]'$$

where δw_{com} are some positive numbers and represent the command for additional weight and the system was simulated with these new parameters. Figure 18 through Figure 23 show the plot of this simulation. In this case, pitch angle reaches a maximum value of 0.18 rad (10.31 degrees) which is 4 times greater than the previous simulation. With increasing pitch angle, there is also an increase in the depth rate. The depth rate becomes 0.35 ft/sec which is again almost 4 times greater than the previous simulation. Since the commanded depth for the control law is the depth of the ground, the system tries to make the vehicle neutrally stable to keep the vehicle on that depth by pumping water out of ballast tanks. After grounding, pumps should pump water in ballast tanks until they are full. Because this additional weight is needed to keep the vehicle sitting on the ground against the current.

Another method for increasing the depth rate is to command with a depth value that is greater than the actual ground depth. Because in the beginning the error will be higher, the weight controller will produce higher values of flow rate.

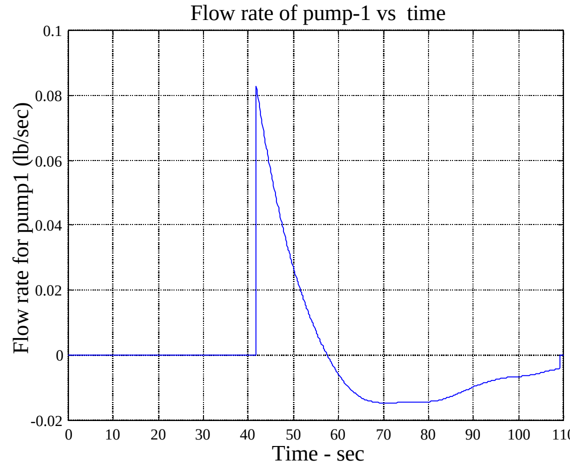

Figure 10. Flow Rate As A Function Of Time For Pump-1 With Depth Command Only

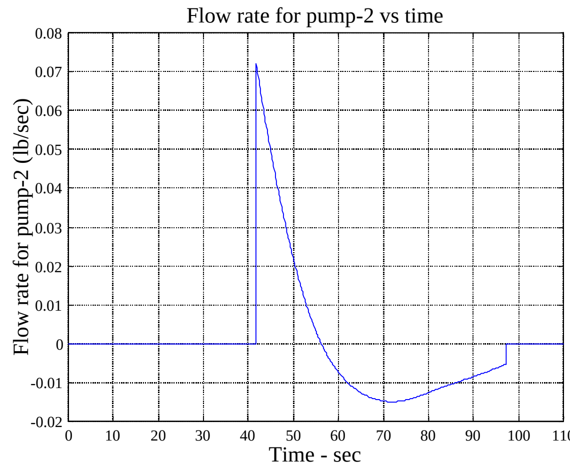

Figure 11. Flow Rate As A Function Of Time For Pump-2 With Depth Command Only

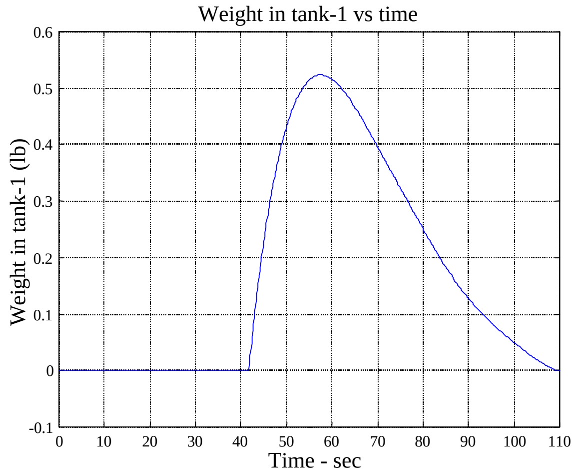

Figure 12. Weight Change In Ballast Tank-1 With Depth Command Only

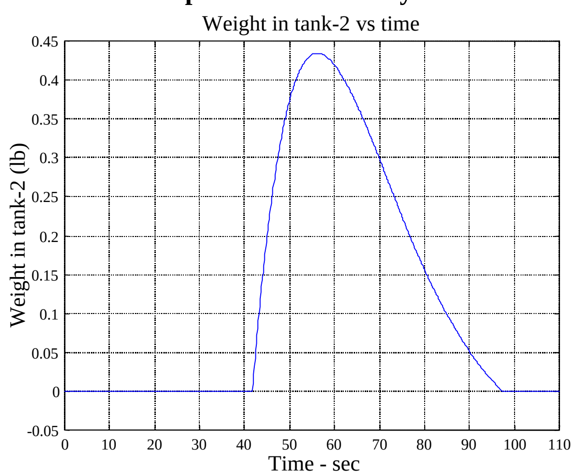

Figure 13. Weight Change In Ballast Tank-2 With Depth Command Only

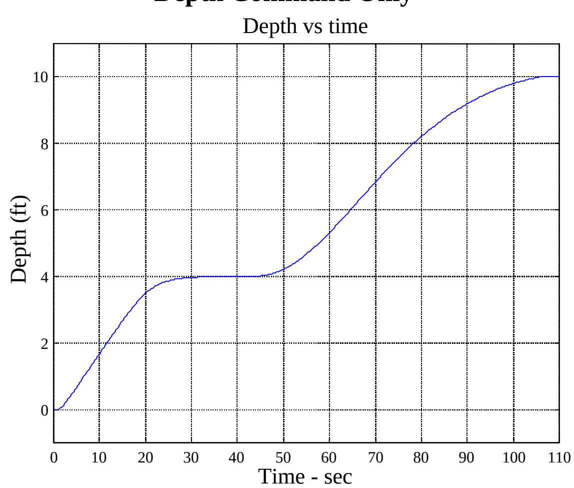

Figure 14. Depth Change During Flight And Grounding

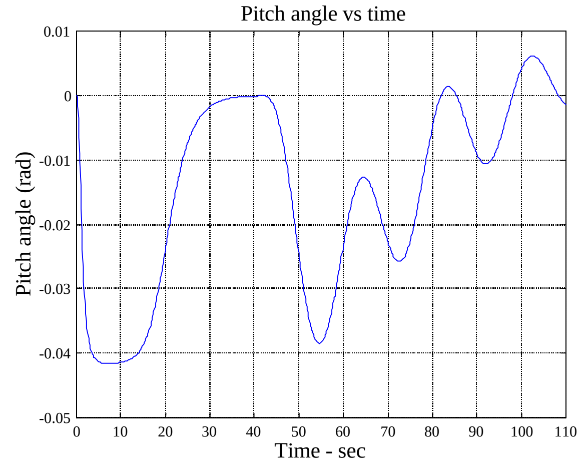

Figure 15. Pitch Angle Change With Depth Command Only

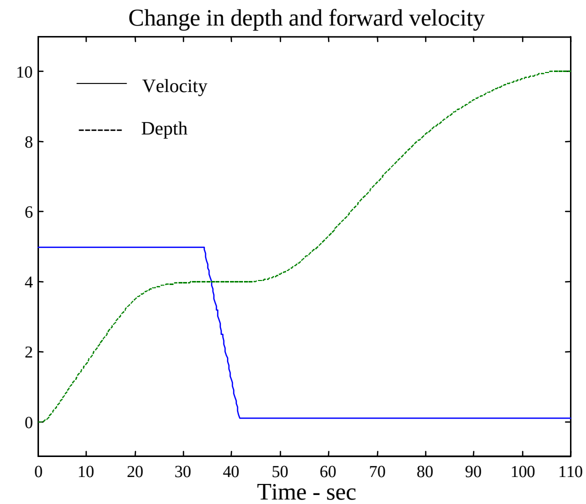

Figure 16. Comparison of Depth and Forward Velocity Change

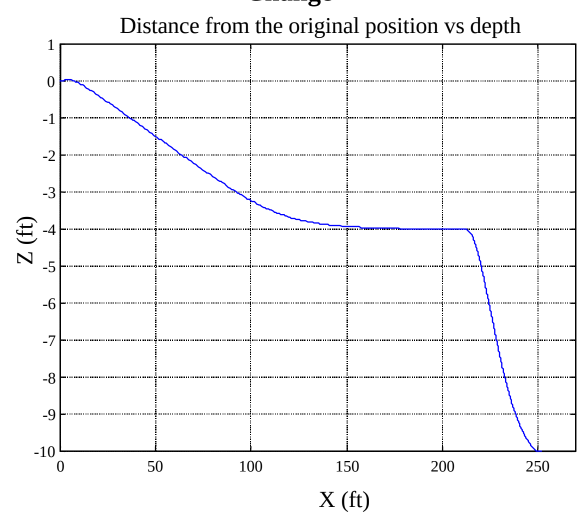

Figure 17. Response Of The Vehicle To The Longitudinal Position Command

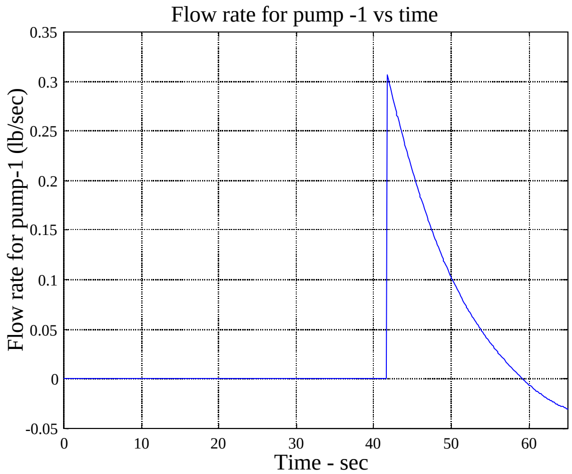

Figure 18. Flow Rate For Pump-1 With Weight And Depth Commands

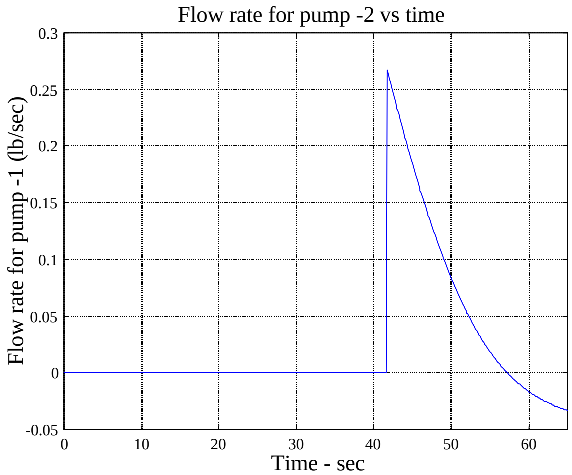

Figure 19. Flow Rate For Pump-2 With Weight And Depth Commands

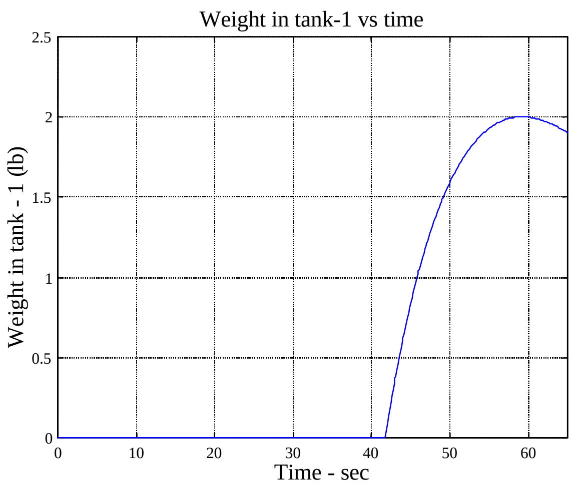

Figure 20. Weight Change In Ballast Tank-1 With Depth And Weight Commands

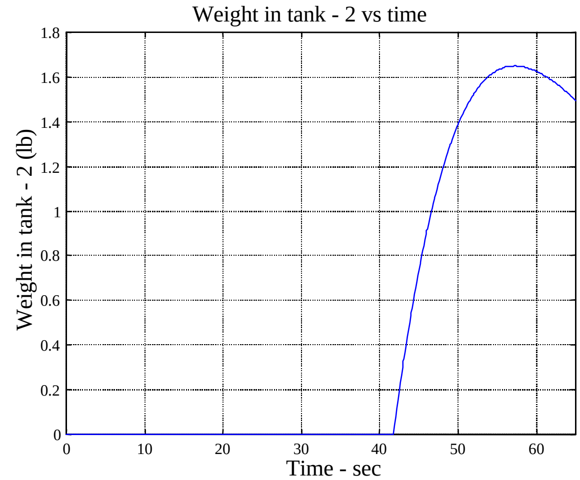

Figure 21. Weight Change In Ballast Tank-2 With Depth And Weight Commands

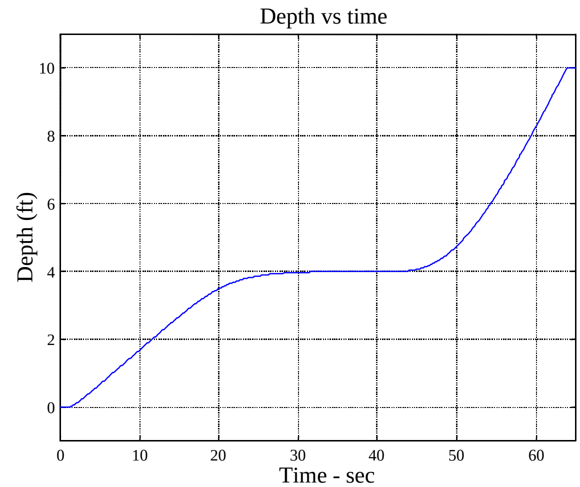

Figure 22. Depth Change With Weight And Depth Commands

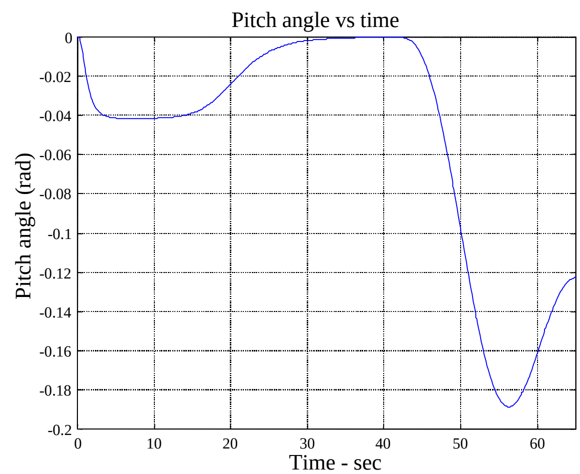

Figure 23. Pitch Angle As A Function Of Time With Weight And Depth Commands

Grounding With Thrusters In Addition To Weight Control

NPS Phoenix AUV's cross-body thrusters consist of a 3 in. ID aluminum tube with a centrally located 4 blade brass propeller. A spur gear is mounted around a 3 in. diameter propeller and driven by a pinion connected to a 24 Vdc motor giving a 2.5:1 gear reduction. The twist of the propeller blade is symmetric enabling bi-directional operation delivering approximately 2.0 pound of bollard pull force in either direction [11]. The system was simulated with the new state equations and the same weight control conditions defined in section C of this chapter. Figure 24 through Figure 29 show the result of this simulation. The depth rate becomes 0.5 ft/sec and the pitch angle reaches a higher value since there is no control on thrusters. Because the thrusters are dominant in this case, the weight controller losses most of its effect on pitch control.

Bottom Stability

The ground also affects the vehicle closing to the bottom. The theory explained by Hoerner and Borst [12], predicts that roughly below C_L =1.5 (C_L represents lift coefficient), lift will be increased in proximity of the ground. Even though no experimental data is provided for NPS Phoenix AUV, it can be assumed that lift coefficient will be less than 1.5. For study of the bottom stability, two different cases of grounding were considered. Figure 30 shows these two cases.

In the case that the vehicle's stern touched to the bottom first, the lift will decrease the weight and increase the angle of attack. This reduces the stability and makes grounding more difficult. But this feature can be very helpful when leaving the ground. In the other case, the bow of the vehicle touches the ground first. This time lift makes the vehicle heavier and decreases the angle of attack providing more stable grounding. After the completion of grounding process, the vehicle sits on the bottom with no lift since the lift coefficient, C_L is assumed zero because of the symmetric shape of the NPS Phoenix AUV. Figure 31 shows the ocean current that the vehicle can stand with different ballast weights sitting on soil with 0.7 friction coefficient. When both ballast tanks are filled with water completely (~23.4 lb. water in each tank), the vehicle can keep its position against 1.52 m/sec (~3 knots) of current.

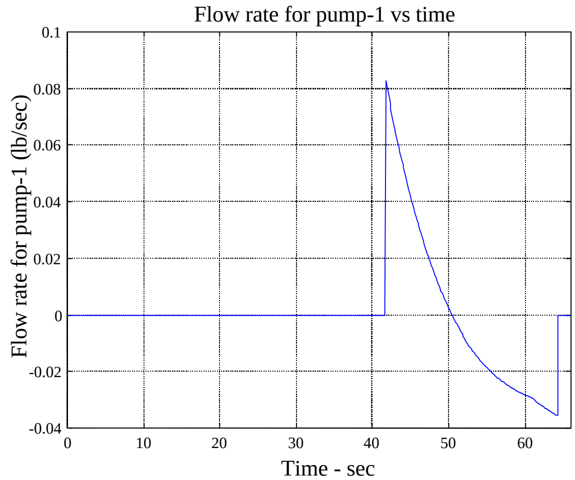

Figure 24. Flow Rate For Pump-1 With Thrusters And Weight Control

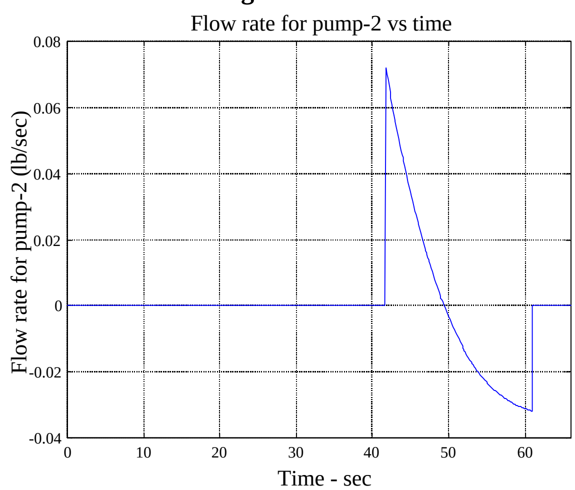

Figure 25. Flow Rate For Pump-2 With Thrusters And Weight Control

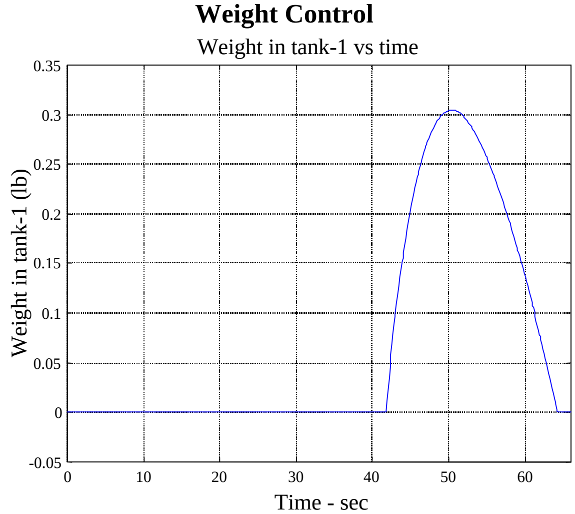

Figure 26. Weight Change In Ballast Tank-1 With Thrusters And Weight Control

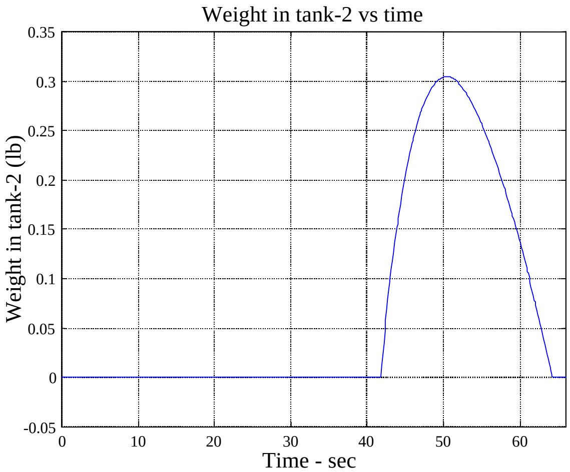

Figure 27. Weight Change In Ballast Tank-2 With Thrusters And Weight Control

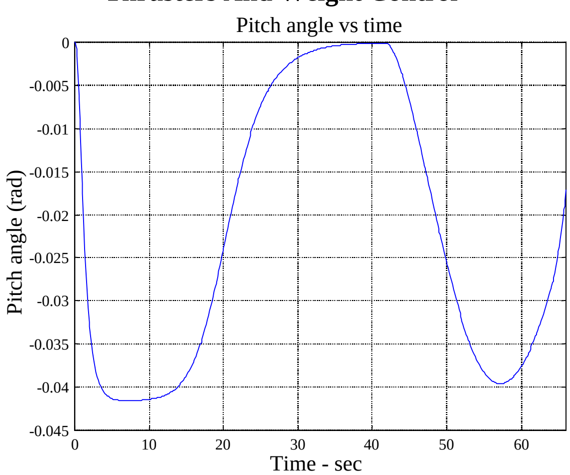

Figure 28. Pitch Angle As A Function Of Time With Thrusters And Weight Control

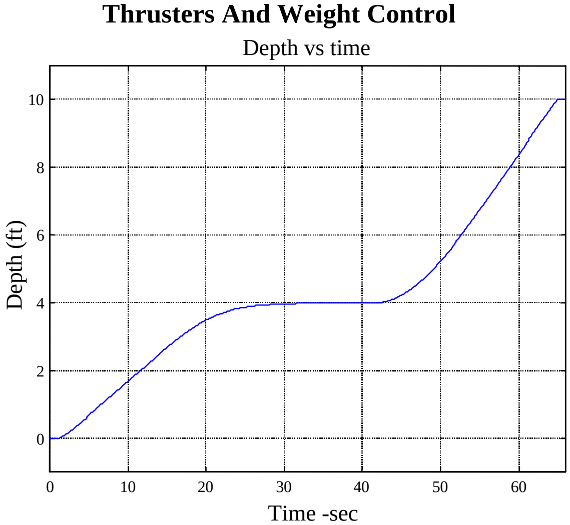

Figure 29. Depth Change During Flight And Grounding With Thrusters And Wt. Cont.

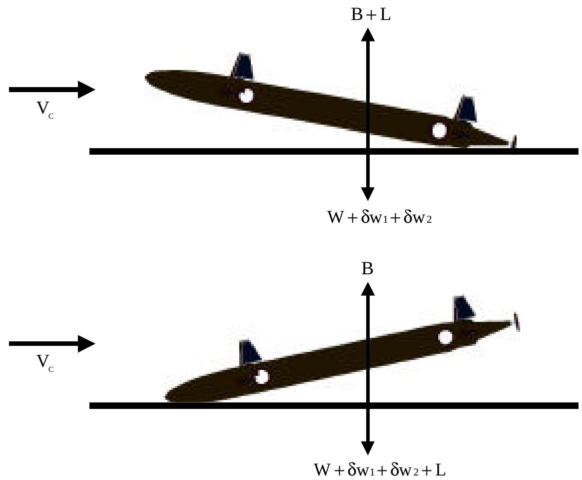

Figure 30. Forces Acting On The Vehicle In Two Cases Of Grounding

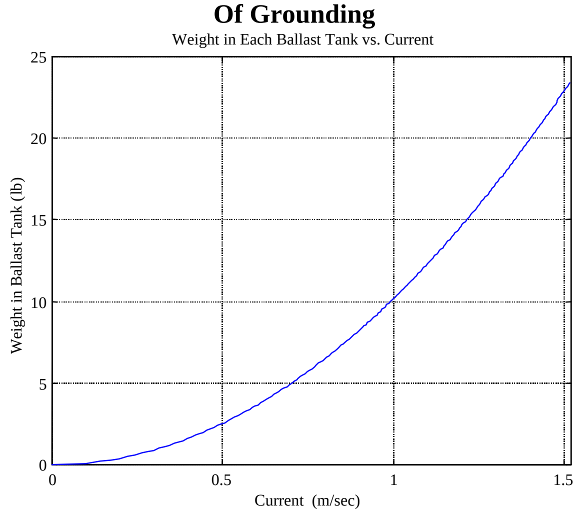

Figure 31. The Current That Vehicle Can Keep Its Position

REFERENCES

1. Schenkenberger, J., "Jens Schenkenberger's Luftschiff Homepage." [http://people. Frankfurt. netsurf.de/Jens.Schenkenberger/]. 1998
2. Motyka, P., and Bergmann, E., "The Design of a Control System for the Ballast and Trim of an Unmanned Submersible", *Proceedings of the 1984 American Control Conference*, San Diego, California, v.3, pp. 1786-1793, 6 June 1984
3. DeBitetto, P.A., "Fuzzy Logic for Depth Control of Unmanned Undersea Vehicles", *IEEE Journal of Oceanic Engineering* , v.20, no.3, pp. 242-247, July 1995
4. Healey, A.J., *Dynamics and Control of Mobile Robotic Vehicles,* Lecture Notes, chp. 2, pp. 3-19, 1995

5. Riedel, J.S., *Pitchfork Bifurcations and Dive Plane Reversal of Submarines at Low Speeds*, Engineer's Thesis, Naval Postgraduate School, Monterey, California, June 1993
6. Papoulias, F.A., *Dynamics of Marine Vehicles*, Lecture Notes, chp. 4, pp 48-61, 1993
7. Hawkinson, T.D., *Multiple Input Sliding Mode Control for Autonomous Diving and Steering of Underwater Vehicles*, Master's Thesis, Naval Postgraduate School, Monterey, California, December 1990
8. Papoulias, F.A., *Modern Control Systems*, Lecture Notes, chp. 6, pp 95-101, 1992
9. Whitcomb, L.L., and Yoerger, D.R., "Comparative Experiments in the Dynamics and Model-Based Control of Marine Thrusters", *Proceedings of the 1995 IEEE Oceans Conference*, San Diego, California, v.1, pp 1019-1028, October 1995
10. Yoerger, D.R., Cooke, J.G., and Slotine, J.E., "The Influence of Thruster Dynamics on Underwater Vehicle Behavior and Their Incorporation Into Control System Design", *IEEE Journal of Oceanic Engineering*, v. 15, no. 3, pp 167-178, July 1990
11. Marco, D.B., *Autonomous Control of Underwater Vehicles and Local Area Maneuvering*, Ph.D. Dissertation, Naval Postgraduate School, Monterey, California, September 1996
12. Hoerner, S.F., and Borst, H.V., *Fluid Dynamic Lift*, chp. 20-21, Mrs. Liselotte A. Hoerner, 1975

ACKNOWLEDGEMENTS

The authors wish to thank the Office of Naval Research for financial support of the NPS AUV program under Work Request N0001498WR30175. This work is based on the MSME thesis of LTJG Bahadir Beyazay, Turkish Navy,